



Universiteit
Leiden
The Netherlands

Baseline fat fraction is a strong predictor of disease progression in Becker muscular dystrophy

Veeger, T.T.J.; Velde, N.M. van de; Keene, K.R.; Niks, E.H.; Hooijmans, M.T.; Webb, A.G.; ... ; Kan, H.E.

Citation

Veeger, T. T. J., Velde, N. M. van de, Keene, K. R., Niks, E. H., Hooijmans, M. T., Webb, A. G., ... Kan, H. E. (2022). Baseline fat fraction is a strong predictor of disease progression in Becker muscular dystrophy. *Nmr In Biomedicine*, 35(7). doi:10.1002/nbm.4691

Version: Publisher's Version

License: [Creative Commons CC BY 4.0 license](https://creativecommons.org/licenses/by/4.0/)

Downloaded from: <https://hdl.handle.net/1887/3276366>

Note: To cite this publication please use the final published version (if applicable).

RESEARCH ARTICLE

Baseline fat fraction is a strong predictor of disease progression in Becker muscular dystrophy

Thom T. J. Veeger¹ | Nienke M. van de Velde^{2,3} | Kevin R. Keene² | Erik H. Niks^{2,3} | Melissa T. Hooijmans⁴ | Andrew G. Webb¹ | Jurriaan H. de Groot⁵ | Hermien E. Kan^{1,3}

¹C. J. Gorter Center for High Field MRI, Department of Radiology, Leiden University Medical Center (LUMC), Leiden, The Netherlands

²Department of Neurology, Leiden University Medical Center (LUMC), Leiden, The Netherlands

³Duchenne Center Netherlands, The Netherlands

⁴Department of Radiology & Nuclear Medicine, Amsterdam University Medical Centers, Amsterdam, The Netherlands

⁵Department of Rehabilitation Medicine, Leiden University Medical Center (LUMC), Leiden, The Netherlands

Correspondence

Thom T. J. Veeger, Leiden University Medical Center, P.O. Box 9600, 2300 RC Leiden, postzone K5-Q, The Netherlands.
Email: t.t.j.veeger@lumc.nl

Funding information

Netherlands Organization for Scientific Research (NWO), Grant/Award Number: 917.164.90; Netherlands Organization for Health Research and Development, Grant/Award Number: 113302001

In Becker muscular dystrophy (BMD), muscle weakness progresses relatively slowly, with a highly variable rate among patients. This complicates clinical trials, as clinically relevant changes are difficult to capture within the typical duration of a trial. Therefore, predictors for disease progression are needed. We assessed if temporal increase of fat fraction (FF) in BMD follows a sigmoidal trajectory and whether fat fraction at baseline (FFbase) could therefore predict FF increase after 2 years (Δ FF). Thereafter, for two different MR-based parameters, we tested the additional predictive value to FFbase. We used 3-T Dixon data from the upper and lower leg, and multiecho spin-echo MRI and 7-T ³¹P MRS datasets from the lower leg, acquired in 24 BMD patients (age: 41.4 [SD 12.8] years). We assessed the pattern of increase in FF using mixed-effects modelling. Subsequently, we tested if indicators of muscle damage like standard deviation in water T₂ (stdT₂) and the phosphodiester (PDE) over ATP ratio at baseline had additional value to FFbase for predicting Δ FF. The association between FFbase and Δ FF was described by the derivative of a sigmoid function and resulted in a peak Δ FF around 0.45 FFbase (fourth-order polynomial term: $t = 3.7$, $p < .001$). StdT₂ and PDE/ATP were not significantly associated with Δ FF if FFbase was included in the model. The relationship between FFbase and Δ FF suggests a sigmoidal trajectory of the increase in FF over time in BMD, similar to that described for Duchenne muscular dystrophy. Our results can be used to identify muscles (or patients) that are in the fast progressing stage of the disease, thereby facilitating the conduct of clinical trials.

KEYWORDS

Dixon, mixed-effects model, MRI, MRS, muscle degeneration/disease progression

Abbreviations used: Δ FF, fat fraction increase at 2-year follow-up; BMD, Becker muscular dystrophy; CSI, chemical shift imaging; DMD, Duchenne muscular dystrophy; EPG, extended phase graph; FF, fat fraction; FFbase, baseline fat fraction; FSHD, facioscapulohumeral dystrophy; GNE, UDP-N-acetylglucosamine 2-epimerase/N-acetylmannosamine kinase; MEM, mixed-effects model; MESE, multi-echo spin-echo; PDE/ATP, phosphodiester over ATP ratio; PROM, patient-reported outcome measure; ROI, region of interest; SI, signal intensity; stdT₂, standard deviation T₂.

This is an open access article under the terms of the [Creative Commons Attribution](https://creativecommons.org/licenses/by/4.0/) License, which permits use, distribution and reproduction in any medium, provided the original work is properly cited.

© 2022 The Authors. *NMR in Biomedicine* published by John Wiley & Sons Ltd.

1 | INTRODUCTION

Becker muscular dystrophy (BMD) is caused by mutations in the *DMD*-gene, leading to truncated and reduced levels of the dystrophin protein in muscle.^{1,2} The disease is characterised by variable and progressive muscle weakness, where muscle tissue is replaced by fat and fibrotic tissue.³ The disease progression is relatively slow and highly variable among patients, ranging from patients showing severe symptoms at paediatric age up to cases with mild symptoms in the elderly.^{4,5}

Currently, there is no cure for the disease, but there are several ongoing clinical trials (NCT-03238235, NCT-04585464, NCT-04386304, NCT-03879304 and NCT-04054375). The slow progression and high variability in symptom onset and progression leads to difficulties in the design of such trials, because these limit the chances of observing clinically relevant changes in disease progression within the typical trial duration of 1–2 years.

Muscle fat fraction, measured by quantitative MRI (qMRI) or MRS, is considered as a potential surrogate endpoint in clinical trials in muscular dystrophies.^{6,7} qMRI has been shown to noninvasively, objectively and accurately assess muscle fat fraction with high reproducibility in many muscular dystrophies, including BMD.^{8–10} Moreover, fat fraction correlates with function,^{11,12} can predict future loss of function and clinical milestones in Duchenne muscular dystrophy (DMD),^{13–16} and can potentially capture changes using much smaller sample sizes compared with functional tests.^{15,17} In BMD, the average increase in fat fraction over 2 years is around 0.7%–1.9% for the lower and upper leg,¹⁸ respectively, which is much lower compared with the 3%–7% over 1 year in DMD patients.¹⁵ In addition, BMD shows considerable variability between patients with fat fraction increases after 2 years ranging from –1.0% to 6.4%.^{18,19} With these limited changes and large variability, it is very important to be able to identify key muscles or patients that are likely to show a large increase in fat fraction within the duration of a clinical trial.

There are several candidate MR parameters that could be used to predict fat fraction increase over time, including baseline (at the start of measurement) fat fraction, phosphodiester over ATP ratio (PDE/ATP) obtained from ³¹P MRS,²⁰ tissue pH,²¹ the average water T₂-relaxation time^{22,23} and standard deviation of water T₂ (stdT₂).²⁴ The fat fraction in DMD follows a sigmoidal trajectory with age,^{13,14} which means that the rate of disease progression is not constant over time, but is highest around the middle region of the fat fraction range. As a result of this trajectory, baseline fat fraction is a good predictor for the rate of fat fraction increase over time in DMD. We recently showed that the largest increases in fat fraction over time occurred in BMD patients with a baseline fat fraction of 40%–60%.¹⁸ Therefore, we hypothesise that the fat fraction increase over time in BMD follows the same pattern as in DMD and that baseline fat fraction can therefore predict fat fraction increase. PDE/ATP,²⁰ tissue pH,²¹ average water T₂^{22,23} and stdT₂²⁴ are related to muscle cell/membrane damage and may precede an increase in fat fraction. For instance, in patients with Pompe's disease or GNE (UDP-N-acetylglucosamine 2-epimerase/N-acetylmannosamine kinase) myopathy, higher baseline water T₂ values were positively correlated with larger increases in fat fraction after 1 year.^{25,26}

In this study, we assessed whether the increase in fat fraction in BMD indeed follows a sigmoidal trajectory and that baseline fat fraction can therefore predict the amount of fat replacement in 2 years. Subsequently, we assessed if measures for muscle damage had additional predictive value to baseline fat fraction for the progression of fat replacement after 2 years. To limit the amount of predictors, we only selected PDE/ATP and stdT₂, as these have been shown to be different between BMD patients compared with healthy controls.²⁷ We chose to include stdT₂ and not average water T₂ because muscle tissue is most likely not replaced by fat at the same rate throughout the muscle.¹⁸ If only parts of the muscle show higher T₂ values, resulting in larger std values for T₂, average T₂ might not be as sensitive to subsequent change in fat fraction.

2 | METHODS

2.1 | Subjects

The MRI and MRS datasets from BMD patients used in this study were previously described by Hooijmans et al.²⁷ and van de Velde et al.¹⁸ Briefly, male BMD patients were scanned at baseline and again after about 2 years. Patients were recruited from the Dutch Dystrophinopathy Database and diagnosis was confirmed by genetic testing.²⁸ The study was approved by the local medical ethical committee and written informed consent was given by all patients.

2.2 | MR acquisition

The MRI examinations were performed at 3 and 7 T, as reported in detail by Hooijmans et al.²⁷ and van de Velde et al.¹⁸ Briefly, on the 3-T MR scanner (Ingenia, Philips Healthcare, Best, The Netherlands), scans included a three-point gradient echo Dixon sequence (T_R/T_E/ΔT_E 210/4.41/0.76 ms; NSA 2; flip angle 8°; voxel size 1 x 1 x 10 mm³; slice gap 5 mm; 23 slices) to quantify muscle fat replacement in the upper and lower leg muscles and a multi-echo spin-echo (MESE) multislice sequence (17 echoes; T_R/T_E/ΔT_E 3000/8/8 ms; voxel size 1.4 x 1.8 x 10 mm³; slice gap 20 mm; five slices) to assess water T₂-relaxation times in the lower leg. Upper leg scans were aligned perpendicular to the femur and

lower leg scans to the tibia. On the same day, ^{31}P MRS examinations were performed on a 7-T MR scanner (Achieva, Philips Healthcare, Best, The Netherlands) and included a ^{31}P 2D chemical shift imaging (CSI) scan to assess phosphorus metabolites in the lower leg. This scan was positioned in such a way that one individual voxel was located within a single muscle over the full length of the coil. The 3-T scans were performed using a 16-element receive coil placed on the leg and a 12-element coil in the table under the leg and 7-T scans using a custom-built double-tuned (^{31}P and ^1H) volume coil around the leg.

2.3 | MRI analysis

Water and fat images were reconstructed offline in Matlab 2019b (MathWorks, Natick, MA) from the 3-T Dixon data using an in-house water-fat separation algorithm, described in detail by Hooijmans et al.²⁷ This algorithm is based on a six-peak lipid spectrum.²⁹ Water T_2 -relaxation times were calculated from the MESE data using the approach described by Keene et al.³⁰ Briefly, an extended phase graph (EPG) fitting approach was used, which considered different relaxation times for a single water and a single fat component, and which were fitted with a dictionary method on a voxel-by-voxel basis. This dictionary was created using water T_2 values from 10 to 60 ms. Voxels that fitted on the boundaries of the dictionary were excluded because they could not be physiologically correct.

Images were visually evaluated for bulk motion artefacts and were excluded if these were present. Regions of interest (ROIs) were drawn on the borders of the muscles in five slices for six lower leg muscles and for 10 upper leg muscles using the Medical Image Processing, Analysis and Visualization program (<http://mipav.cit.nih.gov>). The six lower leg muscles consisted of gastrocnemius medialis, gastrocnemius lateralis, soleus, tibialis anterior, tibialis posterior and peroneus. The 10 upper leg muscles were rectus femoris, vastus medialis, vastus lateralis, vastus intermedius, biceps femoris long head, semitendinosus, semimembranosus, adductor magnus, gracilis and sartorius. The slice containing the insertion of the flexor digitorum longus muscle was chosen to be the centre for the lower leg slices. The middle slice for the upper leg was defined as the most proximal slice where the short head of the biceps femoris was still visible. Because the slice gap was larger for the T_2 images, the middle three slices were used for further analyses, which coincided with the middle and outer slices of the five analysed Dixon slices. ROIs drawn on the Dixon image were eroded by two voxels and the ones drawn on the T_2 image were eroded by one voxel, because of the larger voxel size of the T_2 acquisition. Fat replacement per muscle and per slice was quantified by the fat fraction quantified by signal intensity (SI) fat over the summed SI of fat and water: $\text{SI fat}/(\text{SI fat} + \text{SI water})$ and averaged per ROI. From the T_2 maps, the standard deviation of T_2 was calculated per ROI to get a $\text{std}T_2$ per muscle and per slice. ROIs with less than 50% remaining voxels, due to the exclusion of voxels fitting on the physiological boundaries of the dictionary, were excluded. Subsequently, an area-weighted average fat fraction and $\text{std}T_2$ of the five and three slices, respectively, were calculated per muscle. Representative fat fraction and water T_2 maps for two patients in different stages of the disease, reflected by the amount of fat replacement, are shown in Figure 1.

2.4 | MRS analysis

The MRS analysis was previously reported by Hooijmans et al.²⁷ Briefly, the ^{31}P MRS datasets were exported as free induction decays and processed in the time domain using AMARES in the JMRUI software package (version 5; <http://sermn02.uab.es/mrui/>).³¹ All signals were fitted using Gaussian line shapes and the signal of PDE was presented as the ratio over γ -ATP. Representative spectra for two patients in different stages of the disease, as indicated by the amount of fat replacement, are shown in Figure 1.

2.5 | Statistical analysis

A mixed-effects model 1 (MEM1) was used to determine the pattern of temporal progression of fat fraction in BMD. We hypothesised that the association between baseline fat fraction (FFbase) and the increase in fat fraction at the 2-year follow-up (ΔFF) would follow the trajectory of the derivative of a sigmoidal function, a bell-shaped curve. To be able to capture this relationship, with four distinguishably different slopes (zero – positive – negative – zero), up to the fourth (orthogonal) polynomial term for the association between FFbase and ΔFF was added to the model. The model also included the first three polynomial terms as a fourth-order includes all four polynomial terms. For every order we assessed if the fit was significantly better when that order was added to the previous ones. Because in BMD proximal muscles in general are involved earlier than distal muscles,³² both upper and lower leg fat fraction data were used to include data over a larger range of FFbase. To account for varying disease onset between patients and muscles, a by-muscle and by-patient random intercept was added to the model.

In mixed-effects model 2 (MEM2), we assessed if measures for muscle membrane damage ($\text{std}T_2$ and PDE/ATP) had additional predictive value to FFbase for ΔFF . This model only included lower leg data with ΔFF as an outcome variable, and FFbase, $\text{std}T_2$ and PDE/ATP as predictor variables, because no T_2 and ^{31}P data were available for the upper leg. For the association between FFbase and ΔFF , up to the fourth (orthogonal)

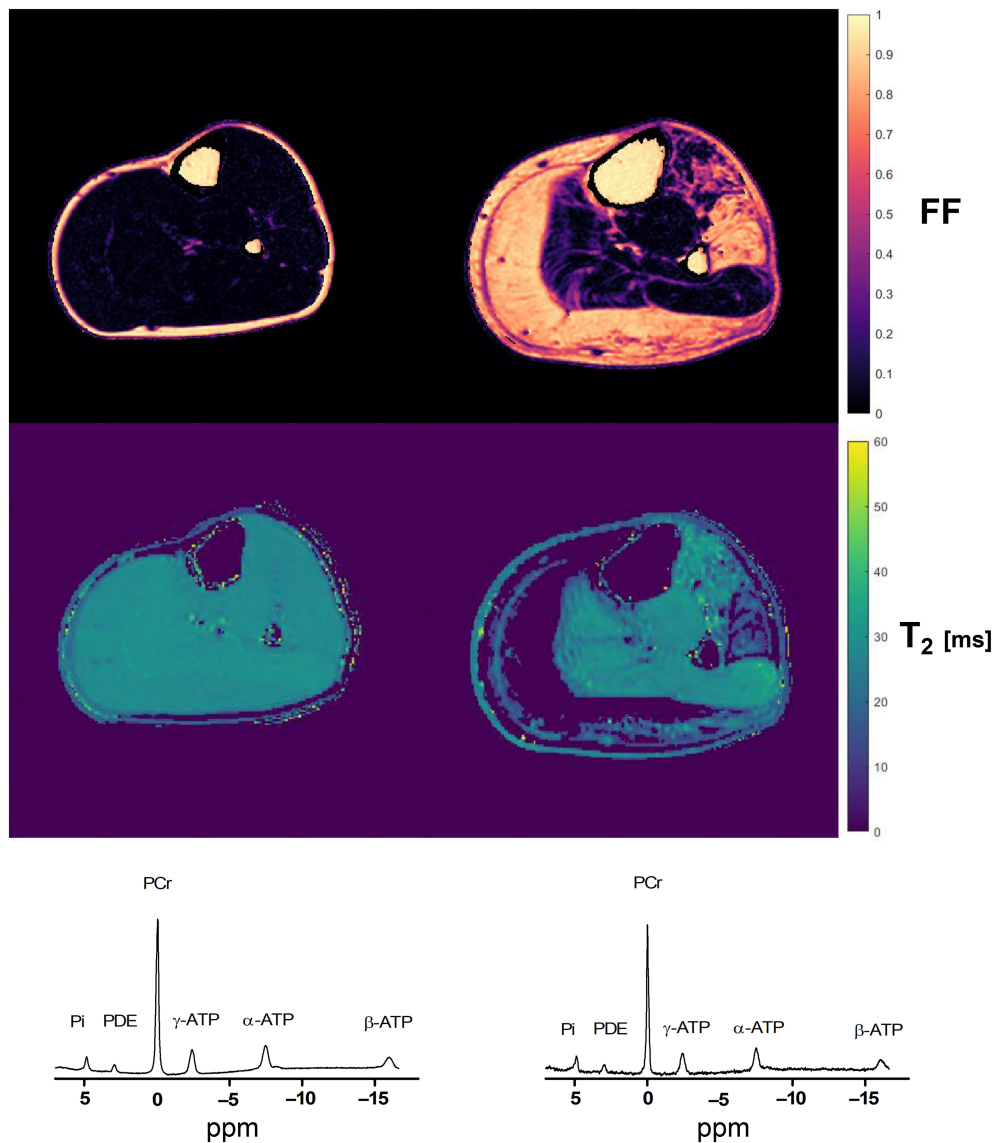


FIGURE 1 Representative fat fraction (upper row), water T_2 maps (middle row) and MRS spectra of the soleus (lower row) for a patient in a relatively early (left column) and relatively late (right column) stage of the disease. For the water T_2 maps, voxels that fitted on the boundaries of the dictionary (i.e., 0 and 60 ms) were excluded, labelled as 0 in these maps. The MRS spectra were fitted in the time domain using Gaussian line shapes and prior knowledge of the linewidths of the PDE and β -ATP.²⁷ FF, fat fraction; PCr, phosphocreatine; PDE, phosphodiester; Pi, inorganic phosphate; ppm, parts per million

order polynomial was added for the association between FFbase and Δ FF (in accordance with the outcome of MEM1). To account for varying disease onset between patients and muscles, a by-muscle and by-patient random intercept was added to the model.

A schematic representation of the workflow can be found in Figure 2. All models and graphs were built using the software package R (R Core Team, 2019) in combination with the packages *lme4*³³ and *visreg*.³⁴ p values for the fixed effects were obtained by t-tests using the *lme4Test* package³⁵ and significance was set at p less than .05. The full code is publicly available at Github (<https://git.lumc.nl/neuroscience/2021-veegertj-sigmoidal-trajectory-bmd>; using the version at commit 466a3b58).

3 | RESULTS

In total, 24 BMD patients participated in this study (Table 1). Data of four patients were missing for follow-up due to death ($n = 1$), implantable cardioverter defibrillator placement ($n = 1$), scan of the wrong leg ($n = 1$) and no show ($n = 1$), and from three patients no usable 7-T MRS data of

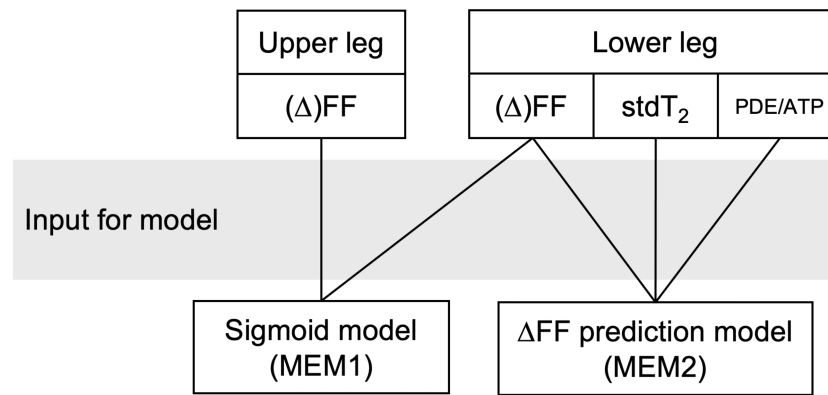


FIGURE 2 A schematic representation of the workflow of the statistical analysis. The upper two rows indicate the type of data available for the upper and lower leg: fat fraction (FF), standard deviation of water T_2 ($\text{std}T_2$) and phosphodiester over ATP (PDE/ATP). The third row refers to the two models and the lines indicate in which models the data were included

TABLE 1 Descriptive statistics

Patients	Number	24
Age (years)	Mean (SD)	41.4 (12.8)
	Range	18.8–68.2
Length (cm)	Mean (SD)	179.1 [*] (7.6)
Weight (kg)	Mean (SD)	77.0 [*] (12.4)
lost ambulation		
Baseline	Number	0
24 months	Number	1

Abbreviation: SD, standard deviation.
^{*}not available for all patients.

TABLE 2 Output mixed-effects model 1

	B (a.u.)	SE B (a.u.)	95% CI (a.u.)	t-value	p value
FFbase – first polynomial	0.139	0.039	0.057–0.217	3.581	<.001
FFbase – second polynomial	–0.296	0.031	–0.358 to –0.234	–9.500	<.0001
FFbase – third polynomial	–0.060	0.031	–0.120–0.001	–1.941	.053
FFbase – fourth polynomial	0.109	0.029	0.051–0.166	3.709	<.001

Note: Significant p values are presented in bold.
 Abbreviation: FFbase, baseline fat fraction.

the lower leg were acquired, because of quality issues. As a result, upper and lower leg data from 20 patients were included in MEM1, with FFbase as predictor of ΔFF , and lower leg data from 17 patients for MEM2, with FFbase, $\text{std}T_2$ and PDE/ATP as predictors of ΔFF .

3.1 | Sigmoidal association between FFbase and ΔFF (MEM1)

The p values in Table 2 indicate whether adding a certain order of the polynomial to the model significantly improved the fit compared with a model only including the previous orders. Thus, the results of MEM1 show that adding the fourth-order term significantly improved the fit of the association between FFbase and ΔFF ($t = 3.709$, $p < .001$). The association is visualised in Figure 3, where the fourth-order polynomial fit is plotted over the data. The fit resulted in a peak ΔFF at around 0.45 FFbase and the lowest ΔFF towards the end of the FFbase range.

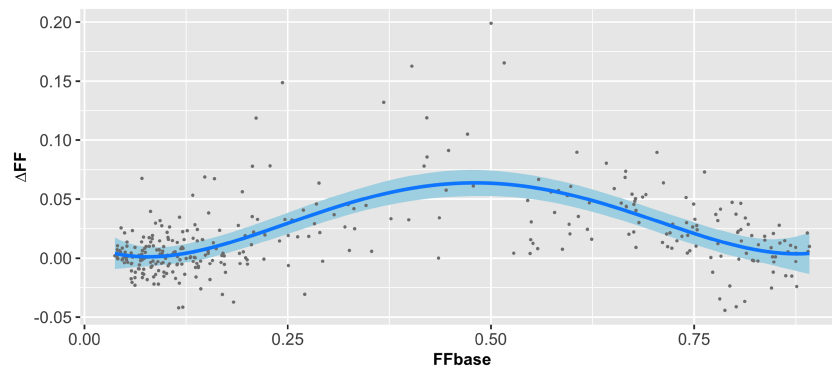


FIGURE 3 Prediction fit (blue line) and 95% confidence interval (light blue band) for the effect of baseline fat fraction (FFbase) on fat fraction increase at 2-year follow-up (Δ FF), including a fourth-order polynomial association. The 340 available datapoints are indicated by the dots. In this analysis, both upper and lower leg data were used

TABLE 3 Output mixed-effects model 2

	B (a.u.)	SE B (a.u.)	95% CI (a.u.)	t-value	p value
FFbase – first polynomial	0.169	0.027	0.109–0.229	6.161	<.0001
FFbase – second polynomial	–0.089	0.019	–0.127 to –0.052	–4.805	<.0001
FFbase – third polynomial	–0.092	0.017	–0.127 to –0.057	–5.413	<.0001
FFbase – fourth polynomial	0.013	0.015	–0.017–0.044	0.866	.389
stdT ₂ (ms)	–0.007	0.007	–0.021–0.006	–1.123	.265
PDE/ATP	0.015	0.023	–0.032–0.068	0.654	.517

Note: Significant *p* values are presented in bold.

Abbreviations: FFbase, baseline fat fraction; stdT₂, standard deviation T₂; PDE, phosphodiester.

3.2 | Predictors for Δ FF (MEM2)

One datapoint of the stdT₂ dataset was marked as an outlier (Z-score = 3.13) and influential point (Cook's distance = 0.50), and was therefore removed from the analysis. The results of MEM2 showed that only FFbase, but neither stdT₂ nor PDE/ATP, significantly predicted Δ FF (Table 3). When inspecting the relationships in more detail, we observed, in line with MEM1, that Δ FF increased with increasing FFbase up to a value of around 0.5, and that with higher FFbase values Δ FF decreased again (Figure 4A). However, in this model the fourth-order polynomial term did not reach significance and therefore did not significantly improve the fit compared with a third-order fit (Table 3). Higher values of stdT₂ showed slightly lower values of Δ FF, although not significantly (Figure 4B, Table 3), and PDE/ATP clearly showed no relationship with Δ FF (Figure 4C, Table 3).

4 | DISCUSSION

We used mixed-effects modelling to test the association between baseline fat fraction and Δ FF at the 2-year follow-up in BMD patients. Subsequently, we analysed whether baseline stdT₂ and PDE/ATP had an additional predictive value to baseline fat fraction when predicting Δ FF. This could help to identify patients or individual muscles that are likely to show a faster progression of the disease within the duration of a clinical trial. Our results showed that the association between baseline fat fraction and Δ FF was described by the derivative of a sigmoid function. Thus, as in DMD, fat replacement of muscles in BMD follows a sigmoidal trajectory. In addition to baseline fat fraction, neither baseline PDE/ATP nor baseline stdT₂ were significantly associated with Δ FF in BMD patients. The slow disease progression in BMD hampers the design of clinical trials, because this limits the chances of observing clinically relevant changes within the typical duration of a trial of 1–2 years. Therefore, there is a need for parameters that are able to identify patients, or key muscles, that are likely to show a faster progression of the disease within the duration of a clinical trial. Our associations indicate that the largest Δ FF after 2 years can be expected in muscles with baseline fat fraction values of around 0.45. This observation, illustrated by a fourth-order polynomial relationship between baseline fat fraction and Δ FF, is in line with our hypothesis that in BMD, as in DMD,^{13,14} the temporal progression of fat fraction follows a sigmoidal trajectory.

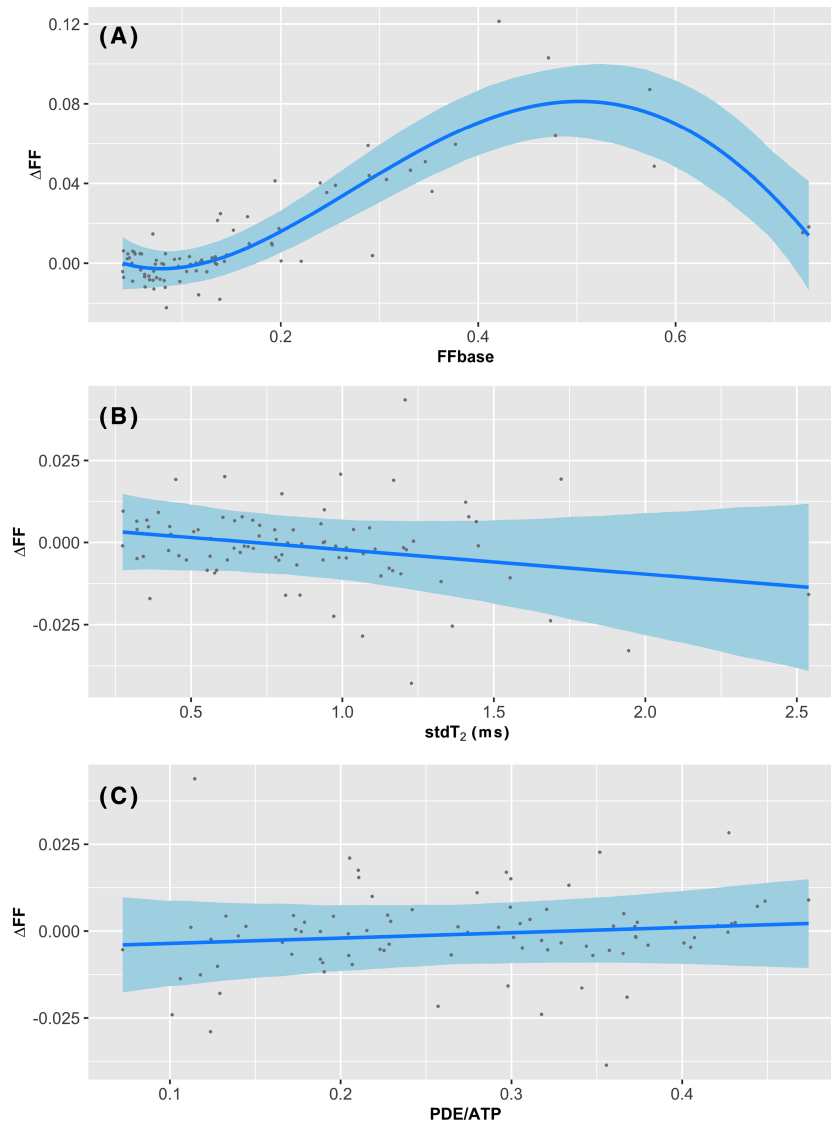


FIGURE 4 Prediction fits (blue lines) for the three fixed effects, (A) Baseline fat fraction (FFbase), (B) Standard deviation of water T_2 ($\text{std}T_2$) and (C) Phosphodiester over ATP (PDE/ATP), and their effect on fat fraction at 2-year follow-up (ΔFF), while keeping the other two variables constant at the median value, with the 95% confidence intervals (light blue bands) and the partial residuals for the 86 available datapoints. In this analysis, only lower leg data were used

The existence of this sigmoidal relationship in BMD is an important finding for both designing clinical trials and interpreting their results. In DMD, it was shown to be helpful for the estimation of important disease progression milestones, such as the age of the patients at which individual muscles would reach a certain fat fraction. For the vastus lateralis muscle in DMD, the age of the patient when it reaches a fat fraction of 0.5 strongly correlates with the loss of ambulation.^{7,13,14} Moreover, it means that averaging the progression over all patients or muscles could mask important effects of a drug or intervention, because patients or muscles in different stages of the disease will show a different magnitude of change. Also, when defining inclusion criteria for a clinical trial, one should try to aim for patients or muscles that are in the fast progressing stage of the disease. Unfortunately, due to the rarity of the disease, selecting BMD patients based on disease stage might not always be feasible, even on an international scale. As an alternative, key muscles for every patient individually could be selected and used as an outcome. This does, however, have the disadvantage that a relation to function or physical function patient-reported outcome measures (PROMs) might be harder to establish.

For baseline $\text{std}T_2$, higher values tended towards lower ΔFF values, although not significantly. The individual correlation with ΔFF , without baseline fat fraction taken into account, suggested that higher $\text{std}T_2$ values were associated with higher ΔFF (data not shown). This indicates that most of the association between $\text{std}T_2$ and ΔFF can be attributed to $\text{std}T_2$ being higher with a higher (baseline) fat fraction, which could be explained by lower T_2 values for muscles with a higher fat fraction.^{30,36}

Baseline PDE/ATP did not have significant predictive value over ΔFF . In addition, when PDE/ATP alone was related to ΔFF , no association was found either (data not shown), suggesting that PDE/ATP has no relation to ΔFF in BMD. This is in agreement with the previously found weak correlation between fat fraction and PDE/ATP.³⁷ It should be noted that there was a difference in coverage between the MRI and MRS acquisition (7 and 12 cm, respectively). Although the ^{31}P coil is indeed 12 cm long, the sensitive region in the long axis is smaller, probably closer to 9 cm, due to the birdcage properties. This results in approximately 0.75 cm extra on both ends of the MRS region. This could result in the inclusion of more fat-replaced muscle regions in the MRS as a result of proximodistal differences.¹⁸ Because it is not clear if all muscles will show more fat replacement towards both ends, we expect only small differences over the complete dataset. Given that we found a negligible association between PDE/ATP and ΔFF , we feel that the small difference in coverage will only have had a limited effect, although we cannot exclude it.

Apart from BMD and DMD, a sigmoidal trajectory of the progression of fat fraction is presumably present in other muscular dystrophies as well, even although it was never formally tested. These include facioscapulohumeral muscular dystrophy (FSHD), spinal muscular atrophy, LGMDR9, GNE myopathy and Pompe's disease.^{25,38-43} For example, in FSHD patients, muscles with intermediate fat fractions occur much less frequently compared with either high or low fat fractions.^{38,39} This is likely a direct result of a sigmoidal trajectory, because there is a smaller time window to select muscles within the intermediate range and thus a smaller chance of randomly including these muscles. In line with our results, in FSHD and LGMDR9, muscles with baseline fat fraction values in the middle range indeed showed a greater increase in fat fraction,^{41,42} and in GNE myopathy similar results were shown, although this was only tested using a linear association.⁴³ By contrast, in Pompe's disease a strong linear relationship between baseline fat fraction and ΔFF was found.²⁵ However, data were averaged over all patients for every upper and lower leg muscle, resulting in mean fat fraction values of up to about 50%, meaning that possibly only the ascending linear part of the curve was fitted. It would be interesting to perform similar analyses as described in the current paper in other muscular dystrophies, to test if a sigmoidal trajectory fat fraction progression can be found in other patient populations as well.

In the current study we did not take the age of the patients into account, while it is highly possible that an interaction effect between baseline fat fraction and age exists. In other words, the slope of the S-curve could be steeper for patients with higher fat fractions at a younger age. Unfortunately, the current dataset contains insufficient individual follow-up observations to test this hypothesis. In future work this could be investigated by acquiring more longitudinal datapoints per patient to fit individual S-curves for each muscle. Consecutively, it could be tested if the slope of these S-curves is associated with the age and disease severity of the patient.

This study has some limitations. First, when only using lower leg data (MEM2), a fourth-order polynomial was not significantly better than a third-order fit. This can be explained by the lack of data in the higher range of baseline fat fractions. Including also upper leg data (MEM1) resulted in a significant fourth-order fit because more datapoints in the higher range of baseline fat fractions were included. Second, a large variance in ΔFF around the peak of the 0.45 baseline fat fraction was observed in both MEM1 and MEM2. This can be explained by the variability in the rate of disease progression between patients and muscles. Baseline fat fraction reflects the stage within the progression when the largest ΔFF can be expected but is not able to predict the amount of ΔFF . In other words, in both slow and fast degenerating muscles, the largest change in fat fraction is expected when the baseline fat fraction is around 0.45.

In conclusion, temporal progression of fat fraction in BMD follows a sigmoidal trajectory because the relationship between baseline fat fraction and the derivative ΔFF could be described by a fourth-order polynomial. Baseline fat fraction can therefore be used to predict fat fraction increase over 2 years, while baseline $stdT_2$ and PDE/ATP did not add significant predictive value. This can be used to identify muscles (or patients) that are in the fast progression stage of the disease.

ACKNOWLEDGMENTS

This work was supported by the Netherlands Organization for Scientific Research (NWO), under research program VIDI (project number 917.164.90), and by the Netherlands Organization for Health Research and Development (113302001).

CONFLICT OF INTEREST

The Leiden University Medical Center and Amsterdam Medical Center are members of the European Reference Network for Rare Neuromuscular Diseases (ERN EURO-NMD).


ORCID

Thom T. J. Veeger  <https://orcid.org/0000-0001-8153-8862>

Nienke M. van de Velde  <https://orcid.org/0000-0002-1541-130X>

Kevin R. Keene  <https://orcid.org/0000-0001-9300-9888>

Erik H. Niks  <https://orcid.org/0000-0001-5892-5143>

Melissa T. Hooijmans  <https://orcid.org/0000-0002-2233-1383>

Andrew G. Webb  <https://orcid.org/0000-0003-4045-9732>

Jurriaan H. de Groot  <https://orcid.org/0000-0002-7828-8863>

Hermien E. Kan  <https://orcid.org/0000-0002-5772-7177>

REFERENCES

1. Bushby KMD, Gardner-Medwin D, Nicholson LVB, et al. The clinical, genetic and dystrophin characteristics of Becker muscular dystrophy - II. Correlation of phenotype with genetic and protein abnormalities. *J Neurol*. 1993;240(2):105-112. doi:10.1007/BF00858726
2. Beggs AH, Hoffman EP, Snyder LR, et al. Exploring the molecular basis for variability among patients with Becker muscular dystrophy: dystrophin gene and protein studies. *Am J Hum Genet*. 1991;49:54-67.
3. Nicolas A, Raguénès-Nicol C, Ben Yaou R, et al. Becker muscular dystrophy severity is linked to the structure of dystrophin. *Hum Mol Genet*. 2015;5:1267-1279. doi:10.1093/hmg/ddu537
4. Andrews JG, Wahl RA. Duchenne and Becker muscular dystrophy in adolescents: current perspectives. *Adolesc Health Med Ther*. 2018;9:53-63. doi:10.2147/ahmt.s125739
5. Zimowski JG, Pilch J, Pawelec M, et al. A rare subclinical or mild type of Becker muscular dystrophy caused by a single exon 48 deletion of the dystrophin gene. *J Appl Genet*. 2017;58(3):343-347. doi:10.1007/s13353-017-0391-8
6. Bonati U, Hafner P, Schädelin S, et al. Quantitative muscle MRI: A powerful surrogate outcome measure in Duchenne muscular dystrophy. *Neuromuscul Disord*. 2015;25(9):679-685. doi:10.1016/j.nmd.2015.05.006
7. Barnard AM, Willcocks RJ, Finanger EL, et al. Skeletal muscle magnetic resonance biomarkers correlate with function and sentinel events in Duchenne muscular dystrophy. *PLoS ONE*. 2018;13(3):e0194283. doi:10.1371/journal.pone.0194283
8. Burakiewicz J, Sinclair CDJ, Fischer D, Walter GA, Kan HE, Hollingsworth KG. Quantifying fat replacement of muscle by quantitative MRI in muscular dystrophy. *J Neurol*. 2017;264(10):2065-2067. doi:10.1007/s00415-017-8547-3
9. Tasca G, Iannaccone E, Monforte M, et al. Muscle MRI in Becker muscular dystrophy. *Neuromuscul Disord*. 2012;22(2):S100-S106. doi:10.1016/j.nmd.2012.05.015
10. Løkken N, Hederemann G, Thomsen C, Vissing J. Contractile properties are disrupted in Becker muscular dystrophy, but not in limb girdle type 2I. *Ann Neurol*. 2016;80(3):466-471. doi:10.1002/ana.24743
11. Barp A, Bello L, Caumo L, et al. Muscle MRI and functional outcome measures in Becker muscular dystrophy. *Sci Rep*. 2017;7:16060. doi:10.1038/s41598-017-16170-2
12. Fischer D, Hafner P, Rubino D, et al. The 6-minute walk test, motor function measure and quantitative thigh muscle MRI in Becker muscular dystrophy: A cross-sectional study. *Neuromuscul Disord*. 2016;26(7):414-422. doi:10.1016/j.nmd.2016.04.009
13. Rooney WD, Berlow YA, Triplett WT, et al. Modeling disease trajectory in Duchenne muscular dystrophy. *Neurology*. 2020;94(15):e1622-e1633. doi:10.1212/wnl.00000000000009244
14. Naarding KJ, Reyngoudt H, van Zwet EW, et al. MRI vastus lateralis fat fraction predicts loss of ambulation in Duchenne muscular dystrophy. *Neurology*. 2020;94(13):e1386-e1394. doi:10.1212/wnl.00000000000008939
15. Willcocks RJ, Rooney WD, Triplett WT, et al. Multicenter prospective longitudinal study of magnetic resonance biomarkers in a large Duchenne muscular dystrophy cohort. *Ann Neurol*. 2016;79(4):535-547. doi:10.1002/ana.24599
16. Barnard AM, Willcocks RJ, Triplett WT, et al. MR biomarkers predict clinical function in Duchenne muscular dystrophy. *Neurology*. 2020;94(9):e897-e909. doi:10.1212/WNL.00000000000009012
17. Nagy S, Schädelin S, Hafner P, et al. Longitudinal reliability of outcome measures in patients with Duchenne muscular dystrophy. *Muscle Nerve*. 2020;61:63-68. doi:10.1002/mus.26690
18. van de Velde NM, Hooijmans MT, Sardjoe Mishre ASD, et al. Selection approach to identify the optimal biomarker using quantitative muscle MRI and functional assessments in Becker muscular dystrophy. *Neurology*. 2021;97(54). doi:10.1212/WNL.00000000000012233
19. Sheikh AM, Rudolf K, Witting N, Vissing J. Quantitative muscle MRI as outcome measure in patients with Becker muscular dystrophy—A 1-year follow-up study. *Front Neurol*. 2021;11:613489. doi:10.3389/fneur.2020.613489
20. Taylor DJ, Kemp GJ, Thompson CH, Radda GK. Ageing: Effects on oxidative function of skeletal muscle in vivo. In: *Detection of Mitochondrial Diseases*. Springer US; 1997:321-324.
21. Reyngoudt H, Lopez Kolkovskiy AL, Carlier PG. Free intramuscular Mg²⁺ concentration calculated using both 31P and 1H NMRs-based pH in the skeletal muscle of Duchenne muscular dystrophy patients. *NMR Biomed*. 2019;32(9):1-13. doi:10.1002/nbm.4115
22. Arpan I, Willcocks RJ, Forbes SC, et al. Examination of effects of corticosteroids on skeletal muscles of boys with DMD using MRI and MRS. *Neurology*. 2014;83(11):974-980. doi:10.1212/WNL.0000000000000775
23. Carlier PG. Global T2 versus water T2 in NMR imaging of fatty infiltrated muscles: Different methodology, different information and different implications. *Neuromuscul Disord*. 2014;24(5):390-392. doi:10.1016/j.nmd.2014.02.009
24. Willcocks R, Arpan I, Forbes S, et al. Longitudinal measurements of MRI-T2 in boys with Duchenne muscular dystrophy: effects of age and disease progression. *Neuromuscul Disord*. 2014;24(5):393-401. doi:10.1016/j.nmd.2013.12.012
25. Carlier PG, Azzabou N, de Sousa PL, et al. Skeletal muscle quantitative nuclear magnetic resonance imaging follow-up of adult Pompe patients. *J Inherit Metab Dis*. 2015;38(3):565-572. doi:10.1007/s10545-015-9825-9
26. Reyngoudt H, Marty B, De Almeida Araújo EC, et al. Relationship between markers of disease activity and progression in skeletal muscle of GNE myopathy patients using quantitative nuclear magnetic resonance imaging and 31P nuclear magnetic resonance spectroscopy. *Quant Imaging Med Surg*. 2020;10(7):1450-1464. doi:10.21037/QIMS-20-39
27. Hooijmans MT, Froeling M, Koeks Z, et al. Multi-parametric MR in Becker muscular dystrophy patients. *NMR Biomed*. 2020;33(11):1-15. doi:10.1002/nbm.4385
28. van den Bergen JC, Ginjaar HB, Van Essen AJ, et al. Forty-five years of Duchenne muscular dystrophy in The Netherlands. *J Neuromuscul Dis*. 2014;1(1):99-109. doi:10.3233/JND-140005
29. Wang X, Hernando D, Reeder SB. Sensitivity of chemical shift-encoded fat quantification to calibration of fat MR spectrum. *Magn Reson Med*. 2016;75(2):845-851. doi:10.1002/mrm.25681
30. Keene KR, Beenakker JM, Hooijmans MT, et al. T2 relaxation-time mapping in healthy and diseased skeletal muscle using extended phase graph algorithms. *Magn Reson Med*. 2020;84(5):2656-2670. doi:10.1002/mrm.28290
31. Naressi A, Couturier C, Castang I, De Beer R, Graveron-Demilly D. Java-based graphical user interface for MRUI, a software package for quantitation of in vivo/medical magnetic resonance spectroscopy signals. *Comput Biol Med*. 2001;31(4):269-286. doi:10.1016/S0010-4825(01)00006-3
32. Emery AEH. Muscular dystrophy into the new millennium. *Neuromuscul Disord*. 2002;12(4):343-349. doi:10.1016/S0960-8966(01)00303-0

33. Bates D, Maechler M, Bolker B, Walker S. Fitting linear mixed-effects models using lme4. *J Stat Softw.* 2015;67(1):1-48. doi:[10.18637/jss.v067.i01](https://doi.org/10.18637/jss.v067.i01)
34. Breheny P, Burchett W. Visualization of regression models using visreg. *R J.* 2017;9(2):56-71. doi:[10.32614/RJ-2017-046](https://doi.org/10.32614/RJ-2017-046)
35. Kuznetsova A, Brockhoff PB, Christensen RHB. Package: tests in linear mixed effects models. *J Stat Softw.* 2017;82(13):1-26. doi:[10.18637/jss.v082.i13](https://doi.org/10.18637/jss.v082.i13)
36. Schlaeger S, Weidlich D, Klupp E, et al. Decreased water T2 in fatty infiltrated skeletal muscles of patients with neuromuscular diseases. *NMR Biomed.* 2019;32(8):e4111. doi:[10.1002/NBM.4111](https://doi.org/10.1002/NBM.4111)
37. Wokke BH, Hooijmans MT, van den Bergen JC, Webb AG, Verschuuren JJ, Kan HE. Muscle MRS detects elevated PDE/ATP ratios prior to fatty infiltration in Becker muscular dystrophy. *NMR Biomed.* 2014;27(11):1371-1377. doi:[10.1002/nbm.3199](https://doi.org/10.1002/nbm.3199)
38. Janssen BH, Voet NBM, Nabuurs CI, et al. Distinct disease phases in muscles of facioscapulohumeral dystrophy patients identified by MR detected fat infiltration. *PLoS ONE.* 2014;9(1):e85416. doi:[10.1371/journal.pone.0085416](https://doi.org/10.1371/journal.pone.0085416)
39. Kan HE, Scheenen TWJ, Wohlgemuth M, et al. Quantitative MR imaging of individual muscle involvement in facioscapulohumeral muscular dystrophy. *Neuromuscul Disord.* 2009;19(5):357-362. doi:[10.1016/j.nmd.2009.02.009](https://doi.org/10.1016/j.nmd.2009.02.009)
40. Otto LAM, Froeling M, van Eijk RPA, et al. Quantification of disease progression in spinal muscular atrophy with muscle MRI—a pilot study. *NMR Biomed.* 2021;34(4):e4473. doi:[10.1002/NBM.4473](https://doi.org/10.1002/NBM.4473)
41. Wang LH, Shaw DWW, Faino A, et al. Longitudinal study of MRI and functional outcome measures in facioscapulohumeral muscular dystrophy. *BMC Musculoskelet Disord.* 2021;22(1):1-11. doi:[10.1186/s12891-021-04134-7](https://doi.org/10.1186/s12891-021-04134-7)
42. Murphy AP, Morrow J, Dahlqvist JR, et al. Natural history of limb girdle muscular dystrophy R9 over 6 years: searching for trial endpoints. *Ann Clin Transl Neurol.* 2019;6(6):1033-1045. doi:[10.1002/acn3.774](https://doi.org/10.1002/acn3.774)
43. Gidaro T, Reyngoudt H, Le Louër J, et al. Quantitative nuclear magnetic resonance imaging detects subclinical changes over 1 year in skeletal muscle of GNE myopathy. *J Neurol.* 2020;267(1):228-238. doi:[10.1007/s00415-019-09569-6](https://doi.org/10.1007/s00415-019-09569-6)

How to cite this article: Veeger TJJ, van de Velde NM, Keene KR, et al. Baseline fat fraction is a strong predictor of disease progression in Becker muscular dystrophy. *NMR in Biomedicine.* 2022;35(7):e4691. doi:[10.1002/nbm.4691](https://doi.org/10.1002/nbm.4691)